Behaviour of single-crystal nickel alloy in the conditions of high-temperature hydrogen corrosion

Pavel Skovorodnikov[1*], *Andrew* Gallyamov[1], *Mustafa* Al-Tameemi[1,2], *Vladimir* Poilov[1], and *Alexander* Kazantsev[1]

[1]Perm National Research Polytechnic University, 29, Komsomolsky prospect, Perm, 614990, Russia
[2]Ministry of Oil-Iraqi Drilling Company, 941, Albarjusia-Zubar, Basra, Iraq

Abstract. This study presents the results of the investigation of the behaviour of ZhS32-VI single-crystal nickel alloy in hydrogen environment or argon atmosphere at 850°C. The microstructure and chemical composition of corrosion deposits were studied by scanning electron microscopy and X-ray energy-dispersive analysis. It has been established that in argon containing an admixture of oxygen a dense scale rich in cobalt and nickel oxides is formed. At atmosphere containing 65% hydrogen and 35% argon an increased content of aluminum in the surface composition was noted. The influence of 100% hydrogen leads to segregation of tungsten and rhenium with the formation of convex growths. The data of simultaneous thermal analysis revealed that the amount of desorbed hydrogen can be from 0.08 to 0.14%.

1 Introduction

As part of the Russian energy system development project and the strategic leadership program has been launched that includes the development of advanced gas turbine technologies the combined commissioning of generating capacities of which can amount to 15-18 GW. The development of the energy program implies to adoption of hydrogen technologies and the use of hydrogen or hydrogen-enriched gas turbine fuel. However, there is a risk to human and technical safety when using hydrogen, since this gas is extremely explosive. Upon that raises the problem of proper fuel preparation and selection of the fuel combustion mode, which will reduce the risks of emergency operation and minimize emissions of harmful substances.

The use of hydrogen as fuel will result in lower mass flow and the formation of flue gases with a high water vapour content [1]. It is known that the reaction products formed during fuel combustion can lead to oxidation and corrosion of alloys [2]. In particular the presence of molecular and atomic hydrogen increases the risk of hydrogen embrittlement or hydrogen corrosion, which will lead to change of alloys plasticity. As the result to

* Corresponding author: pavel.skovorodnikov@yandex.ru

formation cracks and defects in the single-crystal structure of alloys is possible, as well as their growth and branching under mechanical and shock operating loads [3-7].

The course of hydrogen corrosion of alloys can occur according to various mechanisms depending on external (temperature, pressure, flow rate, etc.) and internal (microstructure, phase and chemical composition, the presence of internal stresses) factors. Basically, hydrogen corrosion is isolated as accompanied by the dissolution of hydrogen into the metal with the formation of a solid solution or adsorption by the surface alloy of diffusion-activity hydrogen [8-10]. In this regard, the study of the behaviour of single-crystal nickel alloys under conditions to exposure of hydrogen-containing atmosphere and high-temperature becomes especially relevant. The data of this study can be useful in the development of new alloy compositions resistant to hydrogen corrosion that will improve the technical and economic characteristics of the operation of gas turbine units.

2 Materials and methods

The object of study was a heat-resistant single-crystal nickel alloy consisting of a matrix solid solution of the γ-phase, which has a disordered FCC structure and a heterophase structure of highly dispersed precipitates of the γ′-phase based on an intermetallic compound of nickel with aluminium, which has an ordered FCC structure.

The process of hydrogenation of single-crystal alloy samples was carried out as follows. Samples of heat-resistant alloys were loaded into a tube furnace, then purging with an inert gas or hydrogen was carried out for 15 minutes to completely remove air from the reaction zone. At a given flow rate of hydrogen or hydrogen-containing gas, heating was carried out to the required temperature and exposure was carried out for a given time. After that, the heating was turned off and the samples of alloys in the reaction environment were cooled down to temperature of atmosphere. The diagram of the laboratory setup is shown in Figure 1.

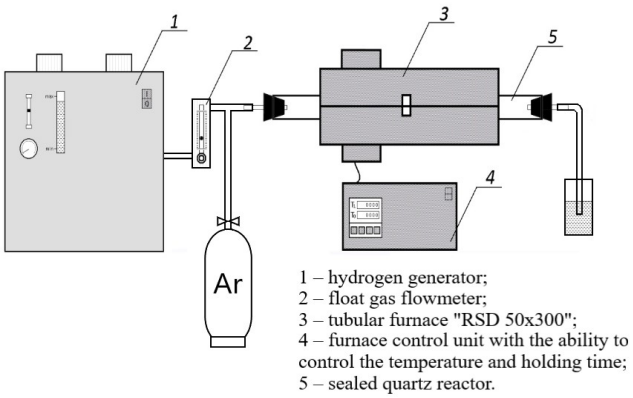

Fig. 1. Diagram of a laboratory installation for testing high-temperature hydrogen corrosion.

3 Results and Discussion

Figure 2 and Table 1 show SEM image and elemental composition of the surface of a single-crystal nickel alloy sample before subjected to hydrogenation process. The distinct crystal structure of the alloy is observed. The provision of oxygen in the composition of the surface of alloy sample was not noted.

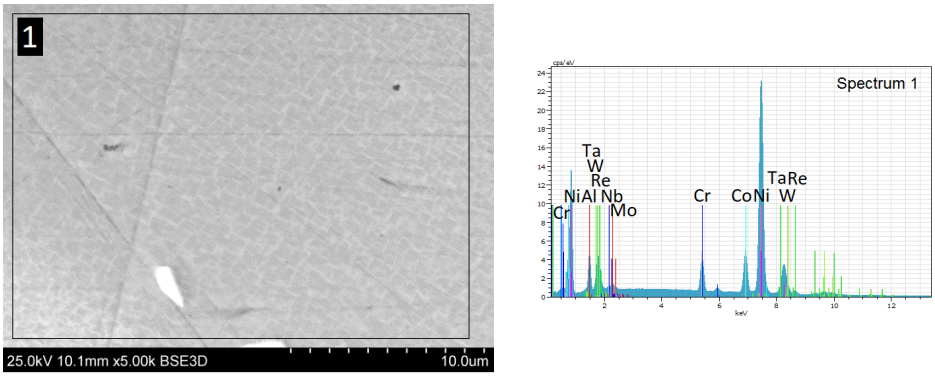

Fig. 2. SEM image of the initial surface ZhS32-VI alloy sample.

Table 1. Content of elements on the initial surface of ZhS32-VI alloy sample.

Spectrum	Content of elements, % mass.									
	Al	Cr	Co	Ni	Mo	Ta	Nb	Re	W	O
1	6.2	5.6	8.2	60.0	1.0	7.6	1.9	3.1	6.4	-

Figure 3 shows SEM image of the surface nickel alloy sample subjected to test at 850°C in argon environment with a purity of 99.0%. The availability of an oxygen impurity in argon caused to oxidation of the alloy surface, as a result to formation of a homogeneous dense oxide scale. According to data in Table 2, it is found that the oxide scale mainly contains nickel, which is the main component of the alloy. An increased content of cobalt was also noted.

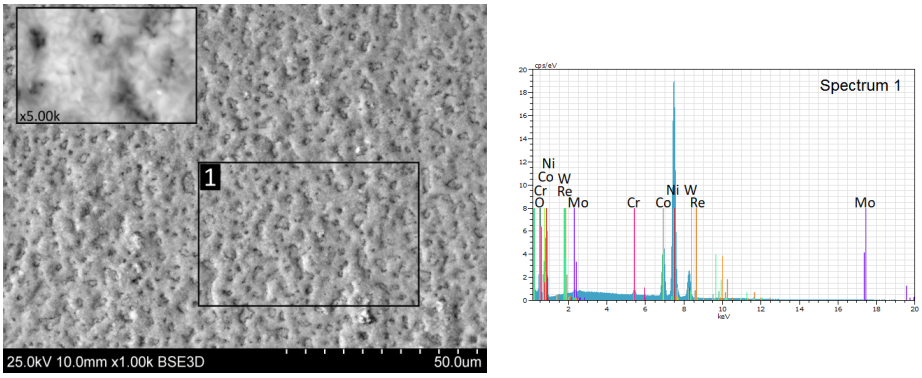

Fig. 3. SEM image of the surface ZhS32-VI alloy sample subjected to test at 850°C in argon (99.0%) environment.

Table 2. Content of elements of the surface of the ZhS32-VI alloy sample.

Spectrum	Content of elements, % mass.									
	Al	Cr	Co	Ni	Mo	Ta	Nb	Re	W	O
100% Ar, 850°C, 4 hour										
1	-	1.0	13.8	63.4	0.7	-	-	0.9	0.6	19.6

Figure 4 shows SEM image of the surface nickel alloy sample subjected to test at 850°C in 35% argon and 65% hydrogen environment. It has been established that oxidation of the alloy predominates, the content of oxygen in the surface composition is 14.7%. However, there is a change in the microstructure of oxide scale due to the influence of hydrogen. The oxide layer is mainly represented by a thin layer of mixed oxide of aluminum and nickel. The surface layer of deposits is presented in the form of micrograins of cobalt and nickel oxides. This phenomenon is associated with a lack of oxygen, which could cause the most intense oxidation and formation of a dense microstructural layer of oxidation products. At the same time, the presence of hydrogen in the reaction environment could cause the opposite effect, leading to the reduction of incomplete metal oxides.

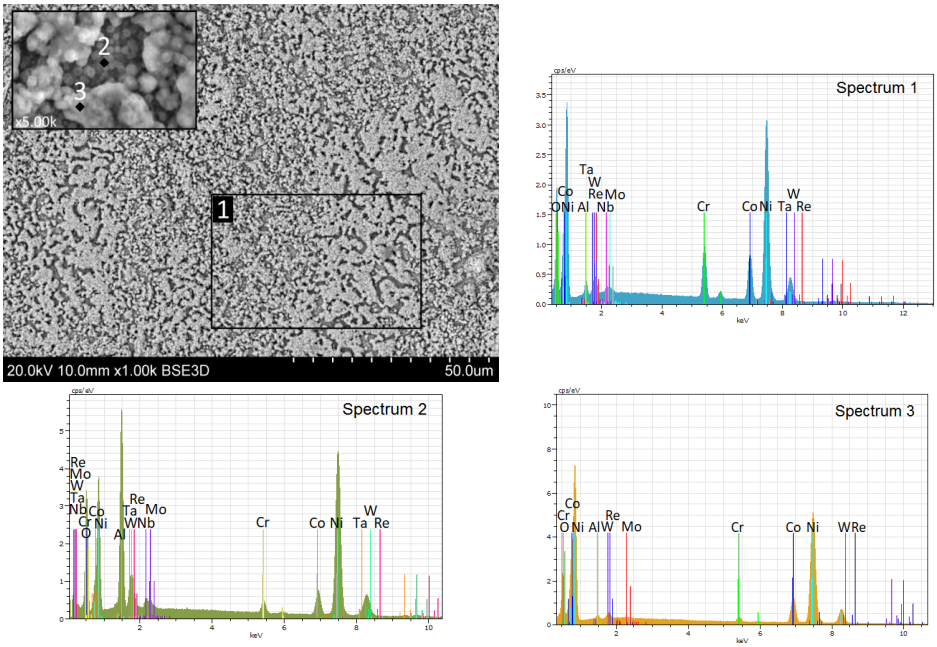

Fig. 4. SEM image of the surface ZhS32-VI alloy sample subjected to test at 850°C in 35% argon and 65% hydrogen environment.

Table 3. Content of elements on the surface of ZhS32-VI alloy sample.

Spectrum	Content of elements, % mass.									
	Al	**Cr**	**Co**	**Ni**	**Mo**	**Ta**	**Nb**	**Re**	**W**	**O**
35% Ar/65% H_2 850°C 4 hours										
1	1.3	7.2	12.4	56.5	0.5	0.1	1.0	1.6	4.7	14.7
2	13.7	1.8	6.7	50.4	0.8	1.8	1.5	0.8	4.7	17.8
3	0.5	1.4	13.4	68.3	0.4	-	-	1.1	2.8	12.1

Figure 5 shows SEM image of the surface nickel alloy sample subjected test at 850°C in 100% hydrogen environment. As a result of the experiment, an insignificant content of oxygen was noted in the composition of the surface, probably this is due to the residual moisture content of hydrogen after the generator. In conditions of a hydrogen-containing atmosphere growths form over the entire surface of the alloy. According to data in Table 4 an increased content of rhenium and tungsten was found in the composition of the growths.

This effect can be associated with the diffusion of alloying elements and segregation of metal particles on the surface.

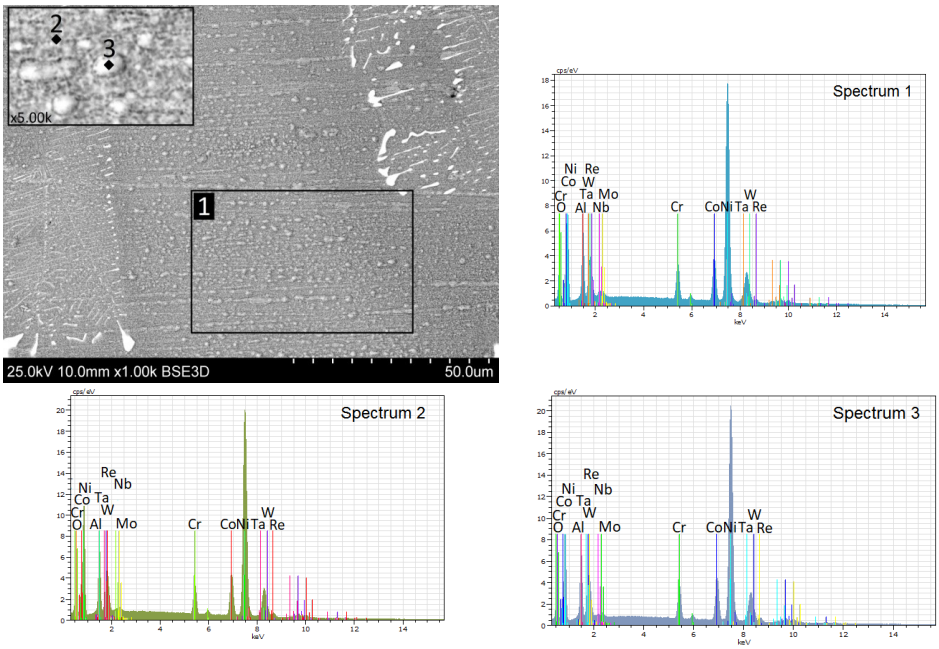

Fig. 5. SEM image of the surface ZhS32-VI alloy sample subjected to test at 850ºC in 100% hydrogen environment.

Table 4. Content of elements on the surface of ZhS32-VI alloy samples.

Spectrum	Content of elements, % mass.									
	Al	**Cr**	**Co**	**Ni**	**Mo**	**Ta**	**Nb**	**Re**	**W**	**O**
100% H_2 850ºC 4 hours										
1	7.8	5.1	9.7	56.3	1.1	2.4	1.6	4.7	10.5	0.8
2	7.4	4.7	10.8	58.2	0.9	0.4	0.4	5.6	11.2	0.4
3	8.0	4.8	10.2	56.5	0.9	0.7	0.6	6.1	11.6	0.6

Since it was difficult to estimate the quantitative content of hydrogen on the surface of the alloy during X-ray analysis due to the impossibility of identification a synchronous thermal analysis was carried. It is known that when the melting temperature of the alloy is reached, hydrogen is desorbed from alloys, as a result of which it is possible to determine the amount of adsorbed hydrogen from the change mass. At the same time metal oxides were not found on the surface of alloy sample after hydrogenation, which could evaporate at high temperature of research and distort the results of synchronous thermal analysis. Thus, to assess the hydrogenation degree of ZhS32-VI single-crystal high-temperature nickel alloy, a simultaneous thermal analysis was carried out on an instrument NETCH model, Germany. Samples before and after hydrogenation were heated to a temperature of 1600°C at a heating rate of 20°C/min in an inert gas flow - argon. The results of

thermogravimetric analysis of ZhS32-VI alloy samples before and after hydrogenation in 100% hydrogen atmosphere at T=850°C for 4 hours are shown in Figures 6 and 7.

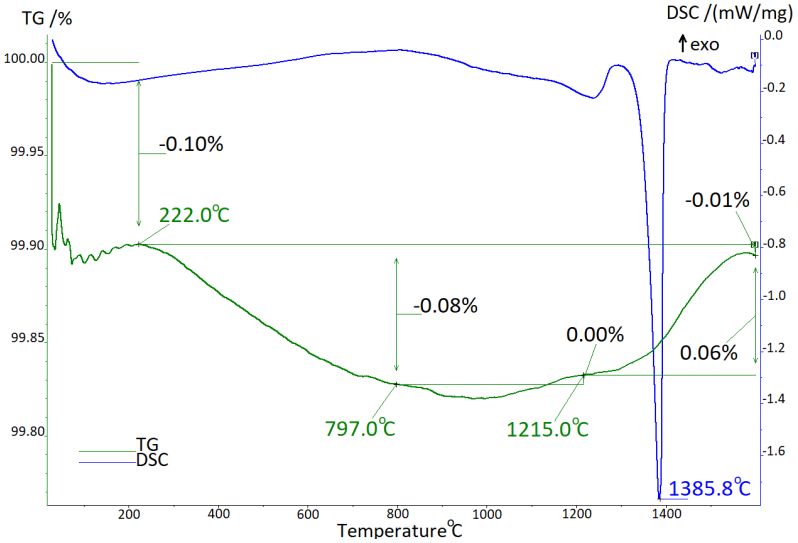

Fig. 6. Thermogram of ZhS32-VI alloy sample before high-temperature hydrogen corrosion.

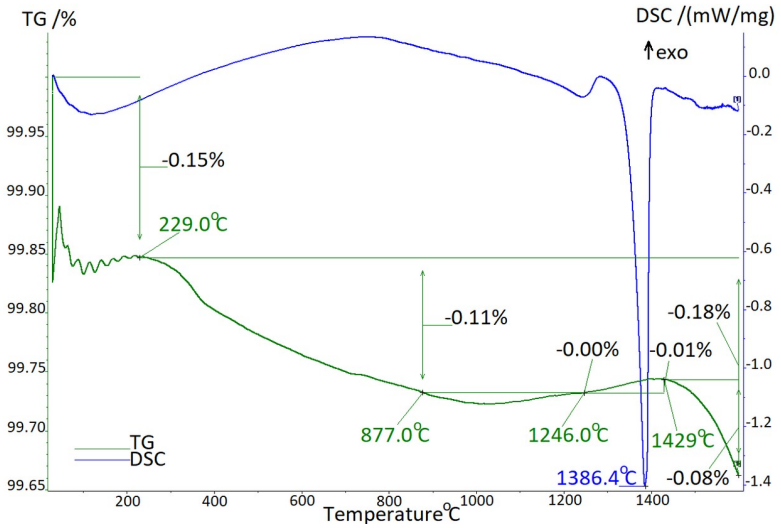

Fig. 7. Thermogram of ZhS32-VI alloy sample after high-temperature hydrogen corrosion.

The TG (thermogravimetric) curve of mass change of alloy sample is green, and the DSC (differential scanning calorimetry) thermal effects curve is blue. The TG curves of ZhS32-VI nickel alloy before and after high-temperature hydrogen corrosion until the melting temperature is reached have the same character. At the initial stage, the removal of adsorbed moisture and gases from the surface of both samples is observed. At 1385.8°C (before hydrogenation) and at 1386.4°C (after hydrogenation) an endothermic effect was noted due to melting of the alloy. After the alloy reaches the state of the melt the curves show differences: in alloy sample before hydrogenation, an increase in the mass by 0.07% is observed, conditioned to oxidation of thermodynamically active metals, such as

aluminum and chromium. After hydrogenation at 1246°C, a slight increase in mass occurs, which stops at a temperature of 1429°C, and a mass loss begins in the amount of 0.08%, which is most likely due to desorption of hydrogen from the melt. Thus, the general amount of hydrogen adsorbed by the surface and dissolved in the volume of the alloy can be 0.08-0.14%.

4 Conclusions

Hydrogen-containing gases at high temperatures lead to formation of different structure deposits and composition on the surface of single-crystal nickel alloy. At low oxygen content a dense microstructural oxide layer rich in cobalt and nickel is formed. At 65% hydrogen containing atmosphere a heterogeneous layer of high-temperature oxidation products with a high content of aluminum in the composition is formed on the alloy surface. At 100% hydrogen atmosphere migration effects of alloying elements - tungsten and rhenium – to the surface of a nickel alloy sample are observed which results in formation of growths.

The result conducted a simultaneous thermal analysis it was found that at melting of a nickel alloy sample at 1429°C there occurs a mass loss of alloy due to the desorption of the adsorbed hydrogen. Since the process of mass loss is prevail over oxidation, which is confirmed by the mass change curves the amount of absorbed hydrogen can be from 0.08 to 0.14%.

Acknowledgement

This research was funded by Ministry of science and higher education of the Russian Federation (Project № FSNM- 2023-0004).

References

1. P. Cheisa, G. Lozza, L. Mazzocchi, J. Eng. Gas Turb. Power-T. ASME, **127**, (2005
2. V.Z. Poilov, A.L. Kazantsev, P.V. Skovordnikov, D.V. Saulin, N.P. Uglev, A.I. Puzanov, Inorg. Mater.: Appl. Res., **13**, (2022)
3. D.F. Johnson, E.A. Carter, J. Mater. Res., **25**, (2010)
4. J. Chen, A.M. Dongare, J. Mater. Sci., **52**, (2016)
5. B. Sun, D. Wang, X. Lu, D. Wan, D. Ponge, X. Zhang, Acta Metall. Sin., **34**, (2021)
6. R.L.S. Thomas, J.R. Scully, R.P. Gangloff, Metall. Mat. Trans. A, **34**, (2003)
7. M. Dadfarnia, A. Nagao, S. Wang, M.L. Martin, B.P. Somerday, P. Sofronis, Int. J. Fract, **196**, (2015)
8. S.P. Lynch, Metall. Mat. Trans. A, **44**, (2013)
9. E. Elmukashfi, E. Tarleton, A.C.F. Cocks, Comput. Mech., **66**, (2020)
10. E.E. Glickman, Metall. Mater. Trans. A, **42**, (2011)